第８回地震時保有耐力法に基づく橋梁等構造の
耐震設計に関するシンポジウム講演論文集（2005 年２月）

SEISMIC PERFORMANCE OF RC COLUMNS UNDER CYCLIC BENDING-TORSIONAL LOADING

Paiboon TIRASIT[1] ・ Kazuhiko KAWASHIMA[2] ・ Gakuho WATANABE[3]

[1]Graduate Student, Department of Civil Engineering, Tokyo Institute of Technology, paiboon@cv.titech.ac.jp
[2]Professor, Department of Civil Engineering, Tokyo Institute of Technology, kawasima@cv.titech .ac.jp
[3]Research Associate, Department of Civil Engineering, Tokyo Institute of Technology, gappo@cv.titech.ac.jp
2-12-1 O-okayama Meguro-ku, Tokyo 152-8550

1. INTRODUCTION

In the urban area, some special bridges, such as C-bent column bridges, skewed bridges and curved bridges, have been constructed because of the limitation of utilized space. During an earthquake, torsion can possibly occur in C-bent columns due to the eccentricity of inertia force transferred from the superstructure. Moreover, the inplane rotation of skewed bridge deck due to the collision with the abutment or adjacent span probably induces twisting moment to the bridge piers. In addition, because the responses of curved bridges in the transverse and longitudinal directions are coupled, the piers are subsequently subjected to the multi-directional deformation with torsion. The combination of seismic torsion and other force components can result in the complex flexural and shear failure in these bridge piers

According to the previous researches, Hsu et al[1] and Hsu et al[2] conducted the experimental studies on the effect of combined cyclic bending and constant torsion on the performance of composite columns with several steel sections. They found that the flexural capacity and ductility of composite columns decreased when a constant torsion was simultaneously applied. Kawashima et al[3] and Nagata et al[4] also conducted a cyclic bilateral loading test and a hybrid loading test on the reinforced concrete C-bent columns, respectively. They revealed that the damage occurred severely on the eccentric compression side and the residual displacement happened in this direction. This resulted from the eccentricity of vertical axial load cooperated with the bending moment and torsion from the eccentric lateral force. Otsuka et al[5] conducted an experimental investigation on the parameters affecting the behavior of reinforced concrete columns under cyclic torsional loading. Their results indicated that the increase of axial force and amount of tie reinforcement could improve the torsional capacity. Otsuka et al[6] also conducted an experimental examination on the combined cyclic bending and torsion on the behavior of reinforced concrete columns. Their results showed that the flexural strength, the ductility and the degree of energy dissipation of columns obviously reduced as the degree of incremental twist angle increased.

However, the knowledge about the interaction between the bending moment and torsion is still limited. The reliable torsional hysteresis model has not been yet available and the behavior of columns under combined cyclic bending and torsion has not been well clarified.

This paper presents a cyclic loading test of 10 reinforced concrete columns to clarify the effect of combined cyclic bending and torsion on the column performance. The primary results about the progress of column failure and the hystereses are discussed.

2. EXPERIMENTAL SETUP

(1) Specimen Properties

Ten reinforced concrete columns with the same configuration as illustrated in Fig. 1 were assembled. The columns had 400mmx400mm square cross section. They were 1750 mm tall and the effective height was 1350 mm. All columns were designed in accordance with the Japanese 1996 Design Specification of Highway Bridges[7]. Type I (middle-

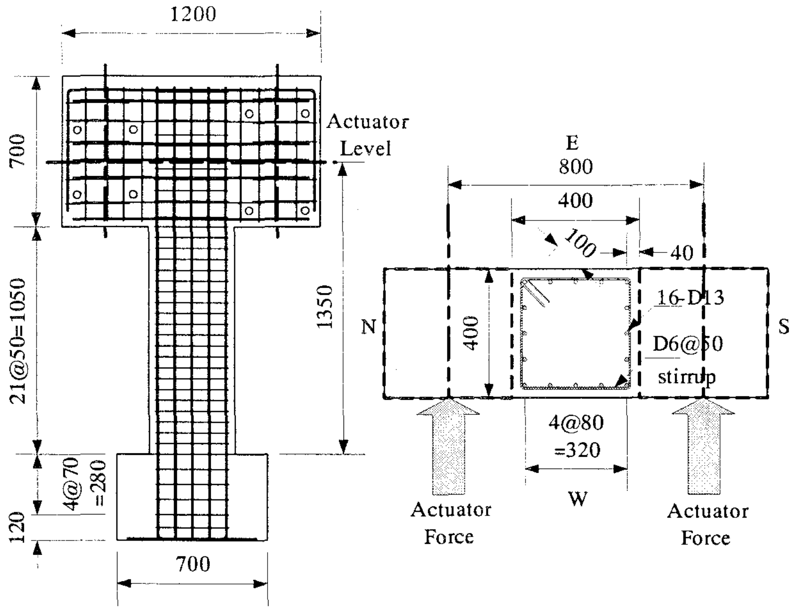

Fig. 1 Specimen configuration

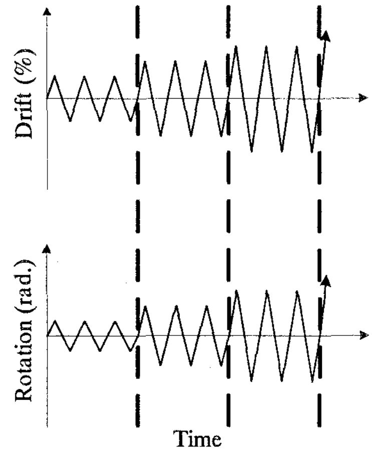

Fig. 2 Loading pattern

Table 1 Experimental cases

Specimen	f'$_c$ (MPa)	Loading Scheme	θ/Δ
P1	31.28	T	∞
P2	28.30	T	∞
P3	25.61	T+P	∞
P4	28.60	M+P	0
P5	32.16	T+M+P	0.5
P6	32.39	T+M+P	1
P7	25.34	T+M+P	1
P8	32.54	T+M+P	2
P9	32.79	T+M+P	2
P10	33.08	T+M+P	4

T: Cyclic torsion

M: Cyclic uniaxial bending

P: 160kN constant axial compressive force

field) and Type II (near-field) ground motion with the moderate soil condition were assumed. The axial stress at the plastic hinge region of the column due to the dead weight of superstructure was assumed to be 1 MPa. The design concrete compressive strength was 30 MPa. Sixteen 13 mm diameter deformed bars with 295 MPa nominal strength (SD295A) were provided as the longitudinal reinforcement. The same grade 6 mm diameter deformed bars were also provided as the stirrups with 50 mm spacing. The longitudinal reinforcement ratio and the tie volumetric ratio were 1.27% and 0.79%, respectively. **Table 1** shows the concrete strength of all columns.

(2) Loadings

Cyclic load test was conducted at Tokyo Institute of Technology. **Table 1** shows the loading conditions of all columns. A constant 160 kN compression was applied to the specimens to produce the 1 MPa axial stress in the plastic hinge region, except columns P1 and P2. The test was conducted under lateral displacement and rotation being controlled. Cyclic torsion and the combined cyclic uniaxial bending moment and cyclic torsion were generated by controlling two horizontal actuators as shown in **Fig. 1**. The effect of axial force on the torsional hysteresis was inspected on columns P1, P2 and P3. Column P4 was tested under cyclic uniaxial bending. Columns P5 to P10 were tested under several combinations of cyclic bending and cyclic torsion which were defined by a ratio of twist angle θ and lateral drift Δ (θ/Δ) as shown in **Table 1**. θ is in radian. **Fig. 2** shows the loading pattern. Each loading step was repeated 3 times.

It is noted that columns P1, P6 and P8 were not in the good condition. The segregation of concrete occurred in columns P1 and P6 because of the insufficient vibrating during construction and the accidental loading from one of horizontal actuators caused some initial cracks in column P8. Due to the space limitation, the results of columns P1, P6 and P8 are not presented here.

3. PERFORMANCE OF COLUMNS

(1) Cyclic torsional loading

Fig. 3 shows the progress of failure of columns P2 and P3 which were under cyclic torsion with and without an axial load, respectively. Under cyclic torsion without an axial load, diagonal cracks were first observed at 0.005 rad twist around the mid

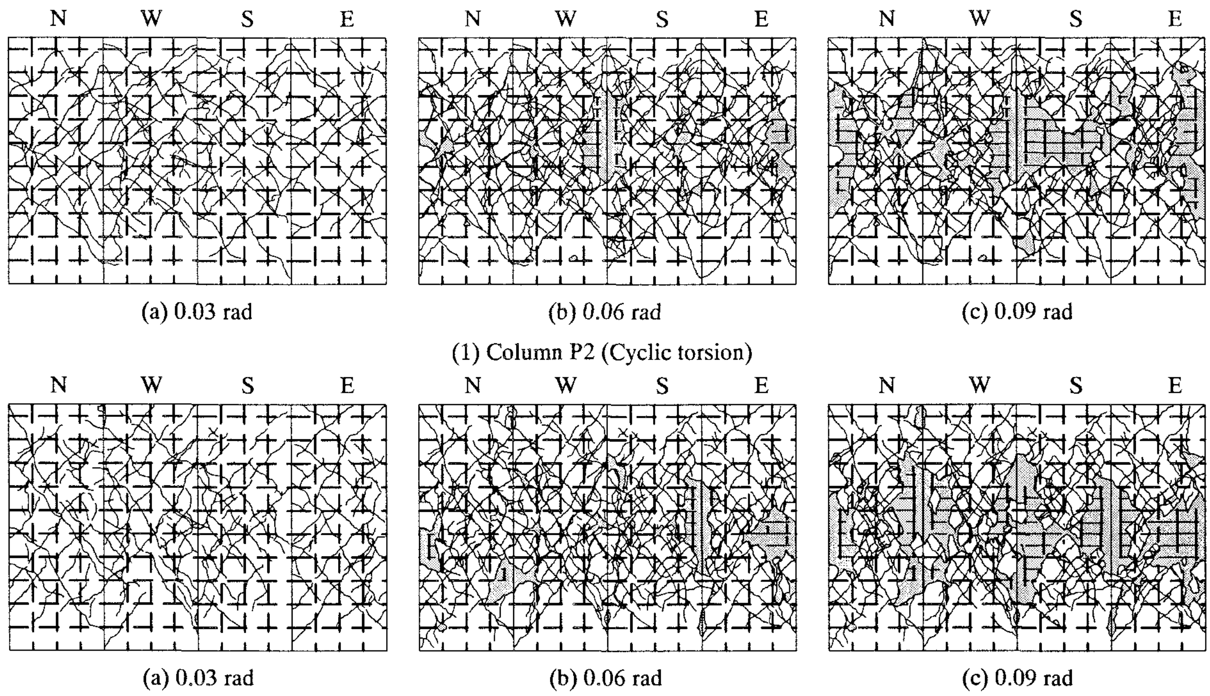

(2) Column P3 (Cyclic torsion under a constant axial force)

Fig. 3 Progress of failure of columns under cyclic torsional loading

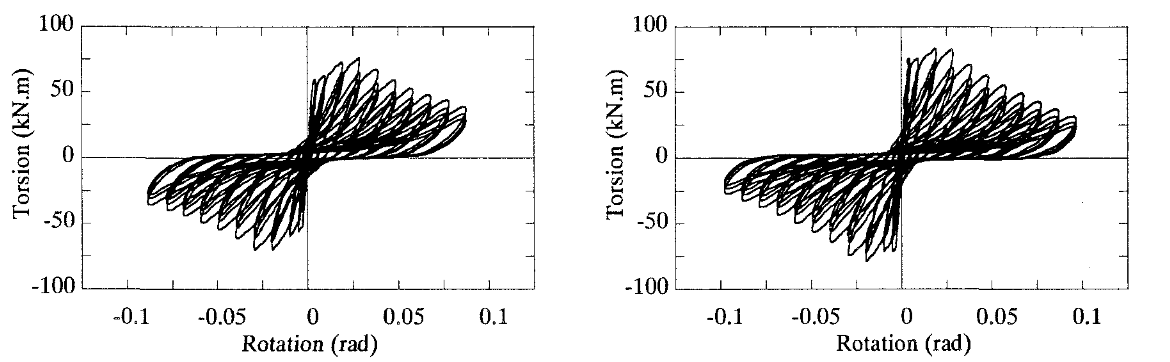

(a) Column P2 (Cyclic torsion)

(b) Column P3 (Cyclic torsion under a constant axial force)

Fig. 4 Torsional hystereses of columns under cyclic torsional loading

height of all column surfaces. The number of cracks increased and propagated over the entire column height as the twist angle increased. The angles of cracks were about 45 degrees with the column cross section. The covering concrete began to spall at 0.03 rad twist. At 0.05 rad twist, the covering concrete deformed outward at the mid height and large covering concrete spalled off at the middle of N-E and S-W corners at 0.06 rad twist. The longitudinal and tie bars were exposed but no buckling took place.

Fig. 4(a) shows the torsional hysteresis of the column subjected to cyclic torsion without axial load. The torsional stiffness remarkably decreased after cracking occurred at 0.005 rad twist. The torsional strength reached 75.8 kN.m at 0.03 rad twist and then gradually deteriorated due to the progress of damage at the middle of column. The restoring force decreased to 77.9% of its strength at 0.05 rad twist.

For the column P3, diagonal cracks were initiated around the mid height on all surfaces at 0.005 rad twist. The column surface started spalling at 0.03 rad twist. At 0.04 rad twist, the covering concrete deformed outward at 500 mm from the footing surface. The covering concrete at S-E corner spalled off at 0.05 rad twist and the longitudinal bars and ties were exposed. Some longitudinal bars slightly buckled outward. Comparing to the column without axial force (P2), the angles of cracks were larger and more extensive damage occurred in column P3.

The torsional hysteresis of the column with axial force is shown in **Fig. 4(b)**. The torsional stiffness sharply deteriorated after cracking at 0.005 rad twist and the column reached its strength of 83.3 kN.m at 0.02 rad twist. This torsional strength was 9.9% larger and occurred earlier than that of column

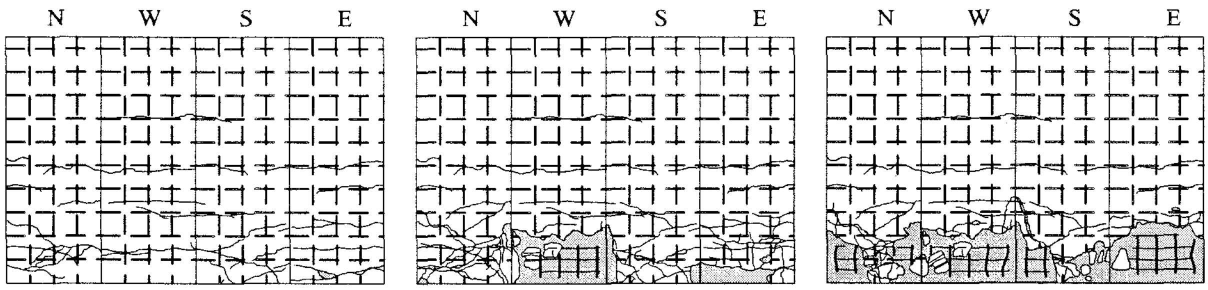

(a) 3.0% drift (b) 4.0% drift (c) 5.0% drift

Fig. 5 Progress of failure of column P4 (Cyclic bending under a constant axial force)

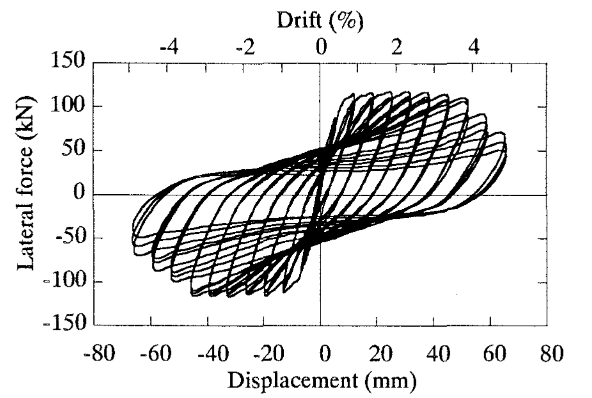

Fig. 6 Flexural hysteresis of column P4 (Cyclic bending under a constant axial force)

without an axial force. Nevertheless, the effect of axial force tended to vanish as the twist angle increased. The restoring force reduced to 75.6% of its strength at 0.05 rad twist.

(2) Cyclic uniaxial bending

The failure progress of column subjected to the uniaxial bending (P4) was shown in **Fig. 5**. The compression failure started to occur in the covering concrete in the plastic hinge region at 3% drift on E surface. The covering concrete began to spall off and the longitudinal and tie reinforcement was exposed at 4% drift. Moreover, buckling occurred in some longitudinal bars at 4.5% drift and the damage further progressed at 5% drift.

Fig. 6 presents the flexural hysteresis of column under cyclic uniaxial bending. The hysteresis reached its maximum capacity of 118.1 kN at 2.5% drift and was stable until 3.5% drift. At 4% drift, the capacity began to deteriorate due to the compression failure of concrete and the buckling of longitudinal steel. The column lost the confinement and its restoring force was 22.2% smaller than its strength at 4.5% drift.

(3) Combined cyclic uniaxial bending and cyclic torsional loading

Several twist angle - drift ratio (θ/Δ) were investigated to clarify the interaction between bending moment and torsion. Their results are demonstrated as followings.

a) $\theta/\Delta = 0.5$

Fig. 7(1) shows the failure progress of column with 0.5 twist angle - drift ratio (P5). Cracks were first observed around the column between 200 mm to 500 mm from the column base at 0.0025 rad - 0.50% drift. The crack formation was nearly similar to that under the uniaxial bending. Cracks, however, did not occur horizontally and there was higher degree of damage in the plastic hinge zone on S surface compared to N surface. This resulted from the larger displacement of actuator on the S side (refer to **Fig. 1**). In addition, only one-directional diagonal cracks occurred on W and E surfaces. The checker board cracks did not take place because of the subtraction between the compressive stress from bending moment and the diagonal tensile stress from torsion. The covering concrete started spalling at 0.0125 rad - 2.5% drift. At 0.015 rad - 3.0% drift, the compression failure occurred in the plastic hinge region on E and W surface. The reinforcement was exposed at 0.02 rad - 4.0% drift. Furthermore, some longitudinal bars began to buckle at 0.0225 rad - 4.5% drift and the damage continuously proceeded at 0.025 rad - 5.0% drift.

The flexural and torsional hystereses of this column are shown in **Fig. 8(1)**. The overall shape of flexural hysteresis was very close to that under cyclic uniaxial bending. The flexural hysteresis reached its maximum lateral force of 118.8 kN at 0.01 rad - 2.0% drift and was stable until 0.0175 rad - 3.5% drift. The flexural restoring force decreased to 70.6% of its strength at 0.0225 rad - 4.5% drift. The torsional hysteresis reached its strength of 38.7 kN.m at 0.005 rad - 1.0% drift, earlier than the occurrence of flexural strength, and gradually reduced to 66.4% of its strength at 0.01 rad - 2.0% drift. However, the influence of torsion was limited.

b) $\theta/\Delta = 1$

The progress of failure of the column with 1 twist angle - drift ratio (P7) is presented in **Fig. 7(2)**. Diagonal cracks were initiated at 0.005 rad - 0.5%

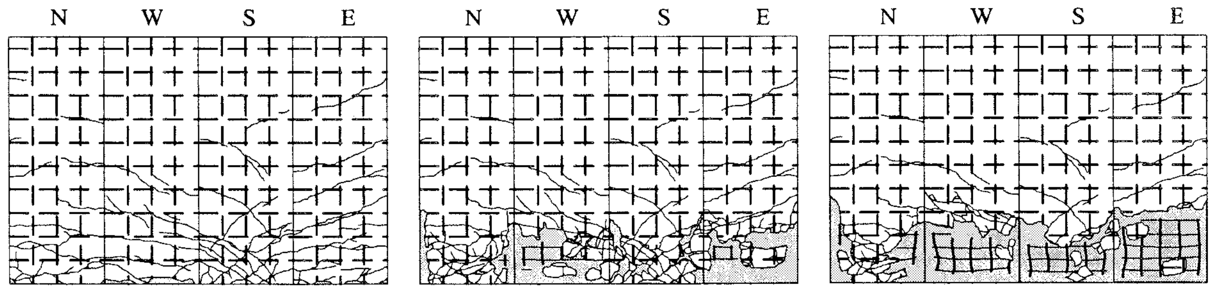

(a) 0.015 rad - 3.0% drift (b) 0.02 rad - 4.0% drift (c) 0.025 rad - 5.0% drift

(1) Column P5 (θ/Δ = 0.5)

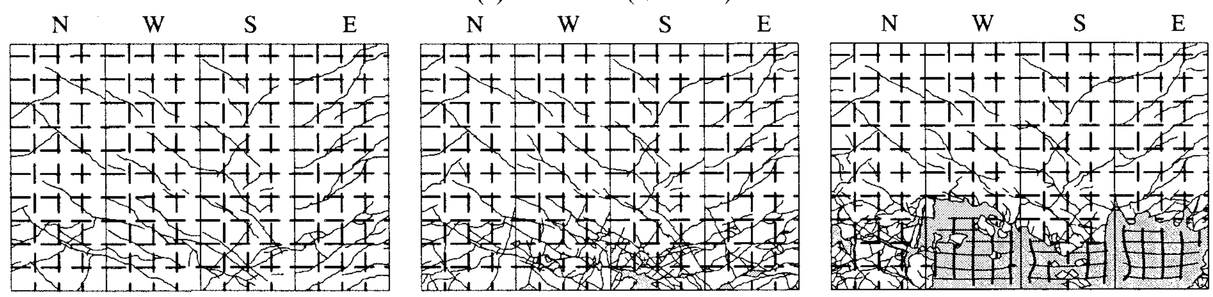

(a) 0.02 rad - 2.0% drift (b) 0.03 rad - 3.0% drift (c) 0.04 rad - 4.0% drift

(2) Column P7 (θ/Δ = 1)

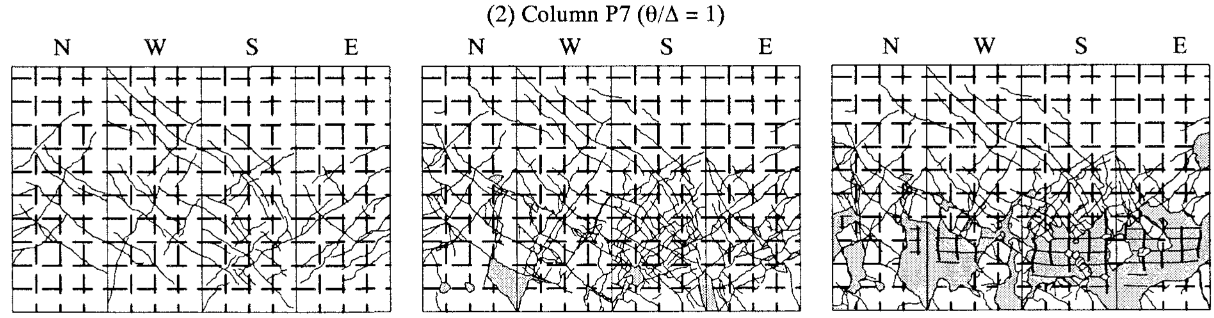

(a) 0.02 rad - 1.0% drift (b) 0.04 rad - 2.0% drift (c) 0.06 rad - 3.0% drift

(3) Column P9 (θ/Δ = 2)

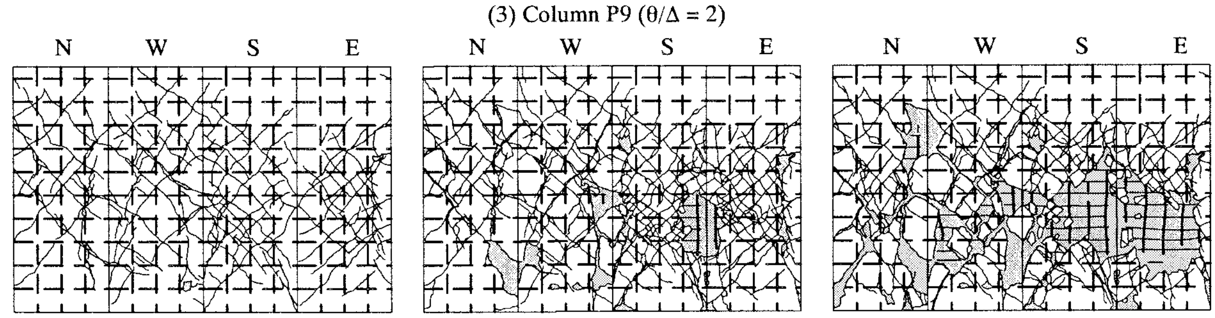

(a) 0.03 rad - 0.75% drift (b) 0.06 rad - 1.5% drift (c) 0.09 rad - 2.25% drift

(4) Column P10 (θ/Δ = 4)

Fig. 7 Progress of failure of columns under combined cyclic bending-torsional loading

drift between 100 mm to 600 mm from the column base on all surfaces and propagated along the column height as the loading level increased. The angles of cracks were larger than those of the column with 0.5 twist angle - drift ratio. However, similarly to the column with 0.5 twist angle - drift ratio, one-directional diagonal cracks occurred on W and E surfaces and S surface suffered more extensive damage than N surface at the plastic hinge region. The covering concrete started spalling at 0.025 rad - 2.5% drift. Consequently, extensive damage occurred on S, E and W surfaces in the plastic hinge zone and the longitudinal bars and stirrups were uncovered at 0.035 rad - 3.5% drift. At 0.04 rad - 4.0% drift, buckling occurred in main bars and finally the column tilted to S direction.

Fig. 8(2) exhibits the flexural and torsional hystereses of the column under 1 twist angle - drift ratio. The column reached its torsional strength of 51.6 kN.m at 0.01 rad - 1.0% drift while it reached the flexural strength of 103.7 kN at 0.02 rad - 2.0% drift. The column flexural capacity was stable until

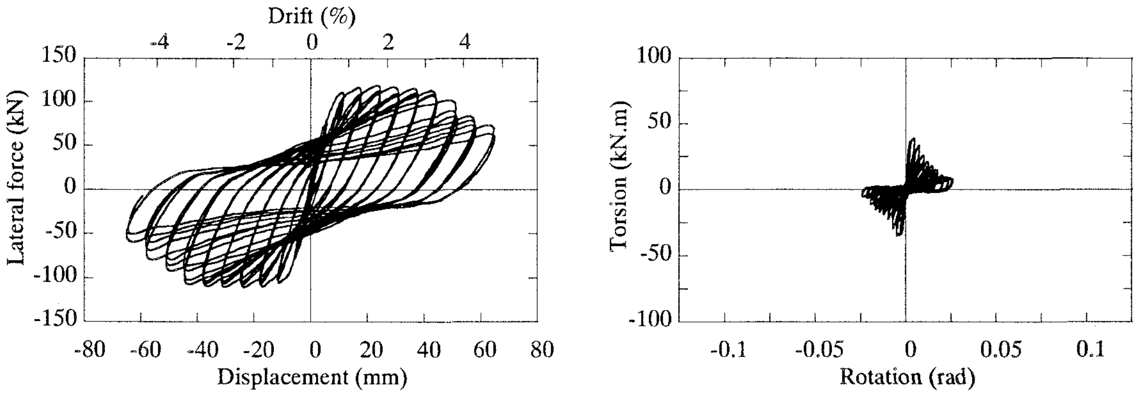

(a) Flexural hysteresis (b) Torsional hysteresis

(1) Column P5 (θ/Δ = 0.5)

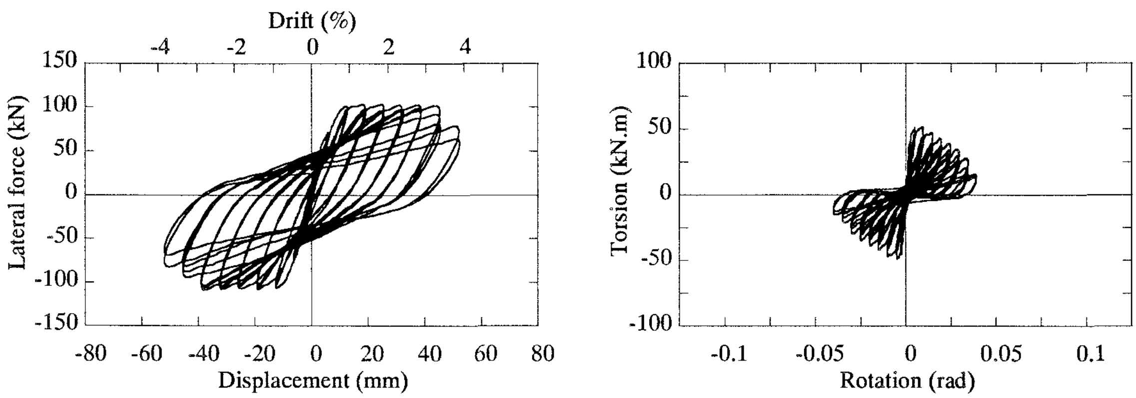

(a) Flexural hysteresis (b) Torsional hysteresis

(2) Column P7 (θ/Δ = 1)

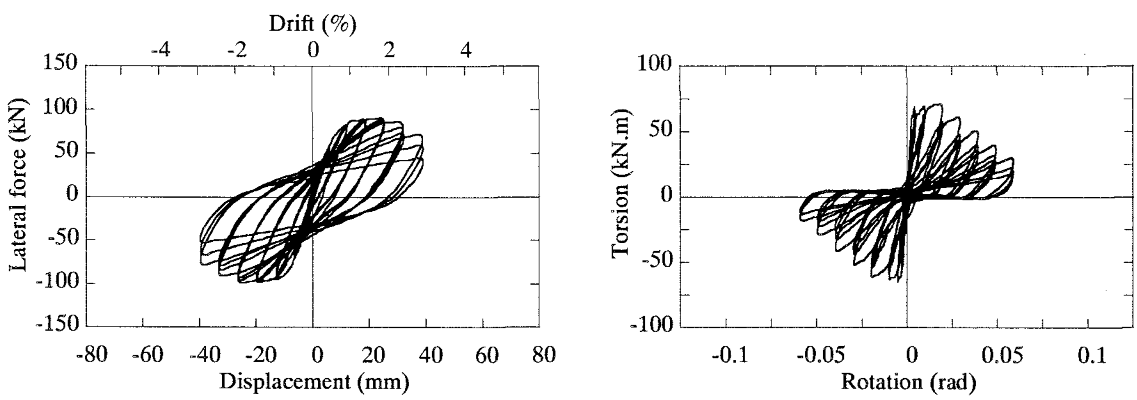

(a) Flexural hysteresis (b) Torsional hysteresis

(3) Column P9 (θ/Δ = 2)

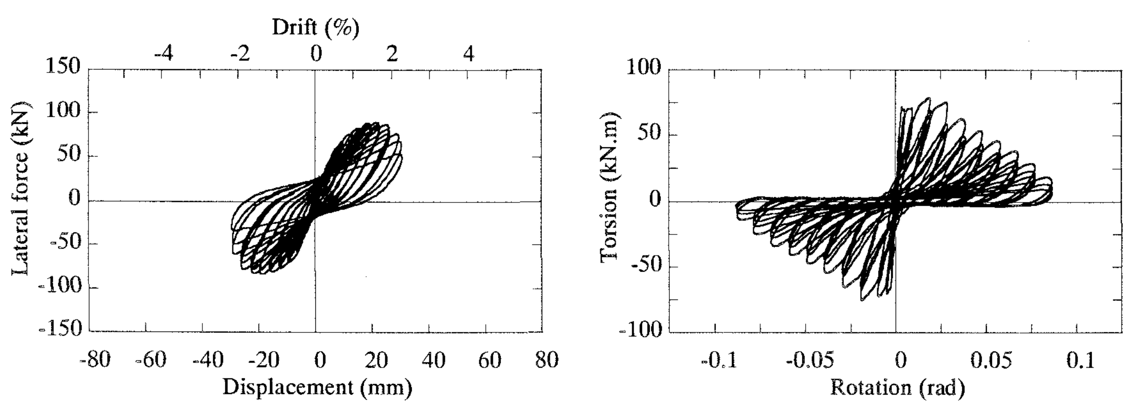

(a) Flexural hysteresis (b) Torsional hysteresis

(4) Column P10 (θ/Δ = 4)

Fig. 8 Flexural and torsional hystereses of columns under combined cyclic bending-torsional loading

0.035 rad - 3.5% drift while the torsional capacity started to deteriorate soon after the peak. The torsional and flexural capacity deteriorated to less than 80% of their strength at 0.025 rad - 2.5% drift and 0.04 rad - 4.0% drift, respectively. The flexural strength of this column was smaller than that under 0.5 twist angle - drift ratio while the torsional strength of this column was larger.

c) θ/Δ = 2

Fig. 7(3) shows the progress of damage of the column with 2 twist angle - drift ratio (P9). Diagonal cracks were first seen at 0.005 rad - 0.25% drift in the range of 100 mm to 600 mm from the bottom on all surfaces. The angles of cracks were larger than those of the former columns with lower twist angle - drift ratio and the checker board cracks developed on all surfaces between 100 mm to 600 mm from the column base. This implies that the effect of torsion becomes predominant. The covering concrete began to spall at 0.03 rad - 1.5% drift. At 0.04 rad - 2.0% drift, the extensive cracks occurred between 100 mm to 600 mm from the column base on S surface. The covering concrete subsequently spalled off excessively and the main reinforcement and stirrups were exposed at 0.05 rad - 2.5% drift. The effect of torsion shifted the location of damage toward outside the plastic hinge zone and shear failure was prevalent. The longitudinal bars buckled and column finally tilted to S direction.

Fig. 8(3) shows the flexural and torsional hystereses of the column with 2 twist angle - drift ratio. The flexural hysteresis reached its strength of 90.8 kN at 0.04 rad - 2.0% drift. This flexural strength was obviously lower than that of the column under cyclic uniaxial bending (P4). The flexural strength suddenly decreased to 79.5% at 0.06 rad - 3.00% drift. On the other hand, the torsional hysteresis reached its strength of 71.4 kN.m at 0.02 rad - 1.0% drift, prior the occurrence of flexural capacity. After that the torsional capacity progressively deteriorated to 70.6% of its strength at 0.04 rad - 2.0% drift.

d) θ/Δ = 4

The progress of damage of the column with 4 twist angle–drift ratio (P10) is shown in **Fig. 7(4)**. The crack formation was close to that of column under cyclic torsion with the axial force. Diagonal cracks were initiated at 0.005 rad - 0.125% drift in the range of 200 mm to 800 mm from the column base on all surfaces. The angles of cracks were larger than those of the previous columns with lower twist angle - drift ratio and the checker board cracks spreaded over the column height. Small spalling of covering concrete took place at 0.03 rad - 0.75% drift. At 0.04 rad - 1.0% drift, the crack width widened and the covering concrete consequently deformed outward at the mid height at 0.05 rad - 1.25% drift. Excessive cracks occurred on S surface and large covering concrete at 200 mm - 500 mm from the base spalled off at S-E corner. Moreover, the longitudinal bars and ties were uncovered. The damage extremely occurred on S, E and W surfaces as the loading displacements increased. The longitudinal steels buckled at 300 mm - 600 mm from the bottom of column.

The flexural and torsional hystereses of the column with 4 twist angle - drift ratio are shown in **Fig. 8(4)**. The flexural hysteresis changed considerably compared to that of the column under cyclic uniaxial bending (P4) while the torsional hysteresis was close to that of column subjected to cyclic torsion with an axial force (P3). The flexural strength was 89.6 kN at 0.07 rad - 1.75% drift while the torsion strength was 79.2 kN.m at 0.02 rad - 0.5% drift. The flexural capacity sharply deteriorated at the first excursion of 0.09 rad - 2.25% drift and became less than 80% of its strength at the second excursion. In contrast, the torsional capacity started to deteriorate soon after the peak and was 79% of its strength at 0.04 rad - 1.0% drift.

3. EFFECT OF COMBINED UNIAXIAL BENDING AND TORSION

Table 2 and **Table 3** summarize the maximum lateral force and torsion, and the ultimate displacement and rotation of the columns, respectively. The ultimate displacement and rotation are defined here as the displacement and rotation where the lateral force and torsion deteriorate to less than 80% of their strengths, respectively. The columns under cyclic uniaxial bending with a constant axial force and under cyclic torsion with a constant axial load are used as the benchmarks. It is apparent that the flexural strength and the ultimate displacement decrease as the twist angle - drift ratio increases. On the other hand, the torsional strength and the ultimate rotation reduce as the twist angle - drift ratio decreases. At the large twist angle - drift ratio, θ/Δ=4, the flexural strength and ultimate displacement are 26.5% and 50% smaller than those of column under cyclic uniaxial bending, respectively.

4. CONCLUSIONS

An experimental study on the effect of combined cyclic bending and torsion on the performance of

Table 2 Maximum lateral force and torsion

Specimen	θ/Δ	Maximum Lateral Force (kN)			Maximum Torsion (kN.m)		
		Positive	Negative	Average	Positive	Negative	Average
P1	∞	-	-	-	71.2	65.2	68.2 (83.9%)
P2	∞	-	-	-	75.8	69.7	72.8 (89.5%)
P3	∞	-	-	-	83.3	79.2	81.3 (100.0%)
P4	0	118.1	116.3	117.2 (100.0%)	-	-	-
P5	0.5	118.8	110.7	114.8 (97.9%)	38.7	34.6	36.7 (45.2%)
P6	1	97.9	103.1	100.5 (85.8%)	47.3	46.7	47.0 (57.8%)
P7	1	103.7	109.0	106.4 (90.7%)	51.6	48.7	50.2 (61.7%)
P8	2	94.4	92.5	93.5 (79.7%)	73.1	66.0	69.6 (85.6%)
P9	2	90.8	98.7	94.8 (80.8%)	71.4	65.0	68.2 (83.9%)
P10	4	89.6	82.6	86.1 (73.5%)	79.2	75.4	77.3 (95.1%)

Table 3 Ultimate displacement and rotation

Specimen	θ/Δ	Ultimate Displacement (% Drift)			Ultimate Rotation (rad)		
		Positive	Negative	Average	Positive	Negative	Average
P1	∞	-	-	-	0.05	0.05	0.05 (100.0%)
P2	∞	-	-	-	0.05	0.05	0.05 (100.0%)
P3	∞	-	-	-	0.05	0.05	0.05 (100.0%)
P4	0	4.5	4.5	4.5 (100.0%)	-	-	-
P5	0.5	4.5	4.5	4.5 (100.0%)	0.01	0.01	0.01 (20.0%)
P6	1	3.5	3.5	3.5 (77.8%)	0.02	0.015	0.0175 (35.0%)
P7	1	4.0	4.0	4.0 (88.9%)	0.025	0.02	0.0225 (45.0%)
P8	2	3.0	3.0	3.0 (66.7%)	0.04	0.04	0.04 (80.0%)
P9	2	3.0	3.0	3.0 (66.7%)	0.04	0.04	0.04 (80.0%)
P10	4	2.25	2.25	2.25 (50.0%)	0.04	0.04	0.04 (80.0%)

reinforced concrete columns was conducted. Based on the results presented herein, the following conclusions may be deduced.

1) Axial compressive force increases the torsional strength of the columns. It also increases the angles of cracks referring to the column cross section. The effect of axial force, however, becomes less as the twist angle increases.

2) Damage in column tends to shift upward from the plastic hinge zone as the twist angle - drift ratio increases. The plastic hinge length, therefore, has to be carefully evaluated for the column under the combined bending moment and torsion.

3) The flexural strength and the ultimate displacement of columns decrease as the torsion increases. In contrast, the torsional capacity and the ultimate rotation reduce as the bending moment increases. Thus, it is essential to take account of this interaction in design of column subjected to the combined flexural and torsional load.

ACKNOWLEDGEMENT: The authors express their sincere appreciation to Messrs. Fukuda, T., Nagai, T., Wang, Y., Ogimoto, H., Kijima, K., Nagata, S., Maruyama, Y. and Ms. Sakellaraki, D. for their extensive support in constructing the columns and executing the experiment.

REFERENCES

1) Hsu, H.-L. and Wang, C.-L.: Flexural-Torsional Behavior of Steel Reinforced Concrete Members Subjected to Repeated Loading, *Earthquake Engineering and Structural Dynamics*, Vol.29, pp. 667-682, 2000.
2) Hsu, H.-L. and Liang, L.-L.: Performance of Hollow Composite Members Subjected to Cyclic Eccentric loading, *Earthquake Engineering and Structural Dynamics*, Vol.32, pp. 433-461, 2003.
3) Kawashima, K., Watanabe, G., Hatada, S. and Hayakawa, R.: Seismic Performance of C-bent Columns Based on A Cyclic Loading Test, *J. of Structural Mechanics and Earthquake Engineering*, No.745/I-65, pp. 171-189, 2003. (In Japanese)
4) Nagata, S., Kawashima, K. and Watanabe, G.: Seismic Performance of Reinforced Concrete C-bent Columns Based on A Hybrid Loading Test, *Proc. of 1st International Conference on Urban Earthquake Engineering*, Tokyo Institute of Technology, Tokyo, Japan, pp. 409-416, 2004.
5) Otsuka, H., Wang, Y., Takata, T. and Yoshimura, T.: Experimental Study on the Parameters Effecting the Hysteresis Loop of RC Members Subjected to Pure Torsion, *J. of Structural Mechanics and Earthquake Engineering*, No.739/V-60, pp. 93-104, 2003. (In Japanese)
6) Otsuka, H., Takeshita, E., Wan, Y., Yabuki, W., Tunumoto, M. and Yoshimura, T.: Study on the Seismic Performance of Reinforced Concrete Columns Subjected to Torsional Moment, Bending Moment and Axial Force, *JSCE J.of Earthquake Engineering*, Vol.27, 67 (CD-ROM), 8 pages, 2003. (In Japanese)
7) Japan Road Association: *Specifications for Highway Bridges - Part V Seismic Design*, Maruzen, Tokyo, 1996.